# Automatic selection of ROI in multispectral imaging of CMS

**Zhang Heng[1], Hu Cuiying[1]*, Meng Qingxia[1], Zhao Jing[2]**

[1]Siyuan Laboratory, Department of Physics, Jinan University, Guangzhou, 510632, Guangdong, China

[2]Department of Applied Physics, South China Agricultural University, Guangzhou, 510642, Guangdong, China

**Abstract.** the multispectral imaging used in identification of Chinese medicine slices (CMS) can identify the authenticity of CMS and evaluate their quality by comparing the characteristic spectral curve from spectral cube. In order to apply multispectral imaging to actual application of CMS identification. Automatically extracting the region of interest (ROI) is necessary. A new algorithm for image segmentation is presented. A mask exactly extracting RIO of the multispectral images is generated by the computer automatically by employing the method. Multispectral imaging experiments with American ginseng and pilose antler were conducted, and the result showed more than 95% of the ROI was extracted using the new algorithm for image segmentation.

**Keywords:** Multispectral Imaging; Chinese medicine slices; Image Segmentation.

## 1 Introduction

The accurate identification of CMS is a basis for evaluating the authenticity and quality of CMS. The traditional detection methods are mainly the character identification, microscopic identification and physicochemical identification [1-3]. The first two need people possessing certain professional knowledge about CMS identification. Physicochemical identification often requires purification, so the method can not be real-time detection, and the process is complex, time-consuming, high-cost, destructive and not repeatable.

Multispectral imaging is an emerging technology that integrates conventional imaging and spectroscopy to attain both spatial and spectral information from a

[1]* Hu Cuiying (✉)
Siyuan Laboratory, Department of Physics, Jinan University, Guangzhou, Guangdong, China
Email: hcyhome@163.com

 

sample. Multispectral imaging was originally developed for remote sensing applications [4] but has since found application in diverse fields such as environment, telemetry, agriculture and other fields [5-7]. The technology has following advantages: without pre-treat, rapid, real-time detection, non-destructive and repeatable. So it has been a technology with strong vitality and attractive. A series of exploratory studies have been conducted about different kinds of CMS by our research group [8-10], and the results show that the multispectral imaging can be used for CMS identification.

Application software, which can automatically process the multispectral data, is required, in order to make multispectral imaging technology can be applied in CMS identification. When multispectral images are selected, the software can automatically complete data calculation and draw the characteristic spectral curve. Among the data processing of the software, selecting the region of interest (ROI) in multispectral images is very important. It can directly affect the characteristic spectral curve, which has a large influence over the accuracy of identification results.

Segmentation method based on the fixed threshold can not meet the needs of automatic segmentation, because the spectral images are very different for different CMS. Filter and pixel location spectrometry[11] can not select ROI accurately, adaptive region growing segmentation method[12] depends on the manual operation on selection growth threshold, and it is difficult to realize automation in data processing. A new algorithm for image segmentation is presented in this paper. It has a strong adaptive ability and can extract ROI of different multispectral images automatically.

## 2 Multispectral imaging system and experiments

### *2.1 Multispectral imaging system*

The multispectral imaging measurement system was self-designed [13]. It is composed of the light source, a light source filter, a liquid crystal tunable filter (LCTF), the controller of LCTF, lens, CMOS sensor, data acquisition card and data processing software. The ray path of the testing system is shown in Fig. 1.

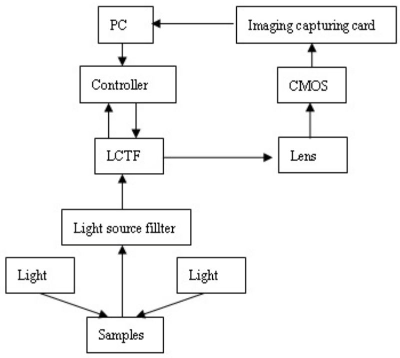


**Fig. 1** The ray path of the system

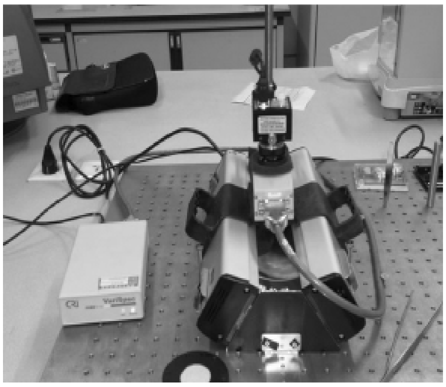

**Fig. 2** Apparatus for multispectral imaging

The excitation light sources are two mercury lamps with the center wavelength of 254 nm in our research. The bandwidth of each lamp is 30 nm, and its optical power is 6w. The samples partially reflect the light coming from the light source after the interaction of light and the sample. The light passes through LCTF carrying the information of the samples. The LCTF is an important component of the system. It is a splitter component based on electrically controlled birefringence of the liquid crystal. The LCTF divides the light and focus it on the image sensor (CMOS). The images are captured by the image acquisition card and saved on the host computer, as JPG format. The two-dimensional spectrum data can be processed and the results are displayed on the monitor of the computer.

## *2.2 Experiments*

The multispectral imaging experiment is performed employing the apparatus depicted in Fig.2 American ginseng and pilose antler are chosen in our experiment.

The samples are put on the underlay directly without any pre-treatment. Single channel, continuous spectrum scan was used in the detection process. The working wavelength of LCTF is from 400nm to 720nm, which is controlled by the controller of LCTF. The wavebands from 400nm to 680nm are chosen in our experiment. The two adjacent frames interval is 5 nm. The spectral resolution is up to 0.5 nm. The CMOS imaging camera was adjusted so that the focal plane coincided with the surface of the test samples at 550nm waveband. The CMOS camera was set to continuous mode with the exposure time of 1000ms, which was synchronized with spectral scanning time, and then the fluorescence images of the test sample were acquired at the whole wavebands. The captured images were stored in the computer with jpg format. A spectral cube of the test sample, formed by 57 frame spectral images, can be obtained in one test. Fig.3 is the spectral cubes of American ginseng and pilose antler.

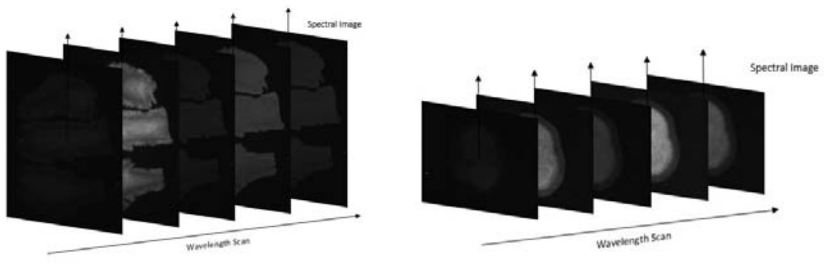


(a) (b)

**Fig. 3** the spectral cubes of (a) American ginseng and (b)pilose antler

## 3 Data analysis and results

### *3.1 Selection of ROI*

Select the ROI in every image to calculate the average light intensity of the corresponding pixel and to normalize them according to equation (1), and then the characteristic spectral curve of the sample can be obtained.

$$\bar{I}_i(\lambda_i) = \frac{\sum_{n=1}^{N} I_{in}(\lambda_i)}{N}. \qquad I_{iNormalized} = \frac{\bar{I}_i(\lambda_i)}{\bar{I}_{i\max}}. \quad (1)$$

Where, N is the number of the pixel, $\bar{I}_i(\lambda_i)$ is average light intensity of the i$^{th}$ image, $i = 1,2,...57$ , $\bar{I}_{i\max}$ is the biggest light intensity among the 57 frame images.

The selection of ROI is the key to data processing. In order to achieve automatic analysis in multispectral imaging, an automatic selection of ROI method is now presented. It can be performed by the following steps:

i. Image difference. In order to enhance the characteristics of ROI and reduce background noise, two images with the maximum gray value and two images with the minimum gray value are chosen. The difference image can be written as:

$$D(x, y) = \frac{1}{2}\left[\left(Max1(x, y)\right) + Max2(x, y)\right] - \frac{1}{2}\left[Min1(x, y) + Min2(x, y)\right] \quad (2)$$

Where, $Max1$ 、 $Max2$ are the images with maximum gray value, $Min1$ 、 $Min2$ are the images with minimum gray value， $D(x, y)$ is differential result. The difference image of pilose antler is illustrated in Fig. 4. Namely, the background noise is eliminated.

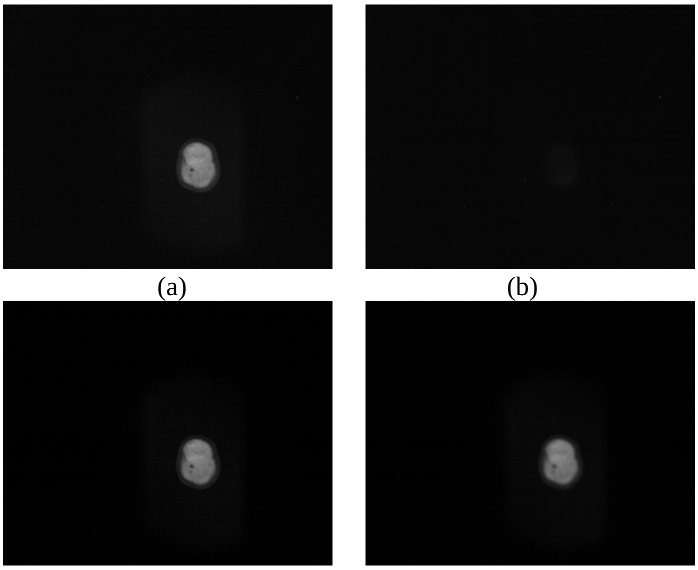

(a) (b) (c) (d)

**Fig. 4** (a) the average gray image of max1and max2, (b) the average gray image of min1and min2,(c) the difference image of (a) and (b), (d) the blurring imaging of (c)

ii. Blurring the difference image. The edge of the ROI in the spectral image of pilose antler is not particularly obvious and there is some dark area in the ROI. In order to automatically choose ROI by the computer, fuzzy processing of the difference image is necessary. Gauss filter is employed and the size of filter window is $5 \times 5$. Fig. 4 (d) is the blurring imaging of (c).

iii. The threshold determination. Since the distribution of gray values for different spectral images are not identical, the threshold, used to select the ROI, is not possible to set a fixed value. The histogram statistics method is employed to achieve self-adaptive selection of ROI for various spectral images. Gauss filter is also used in the processing. The formula is written as:

$$N'(x) = \frac{4}{24}N(x-2) + \frac{5}{24}N(x-1) + \frac{6}{24}N(x) + \frac{5}{24}N(x+1) + \frac{4}{24}N(x+2) \quad (3)$$

Fig. 5 is the histogram statistics before and after Gauss filtering for American ginseng and pilose antler spectral images. As can be seen, the threshold parameter can be uniquely determined by a computer program. Then the ROI can be exactly selected for spectral images. The ROI of American ginseng and pilose antler spectral images are shown in Fig. 6. Compared with their original images, More than 95% of the ROI is extracted.

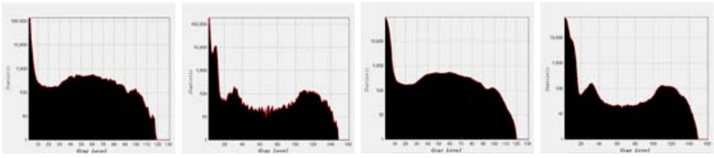

(a) (b) (c) (d)

**Fig. 5** (a) and (b) the histogram statistics before Gauss filtering for American ginseng and pilose antler. (c) and (d) the histogram statistics after Gauss filtering for American ginseng and pilose antler.

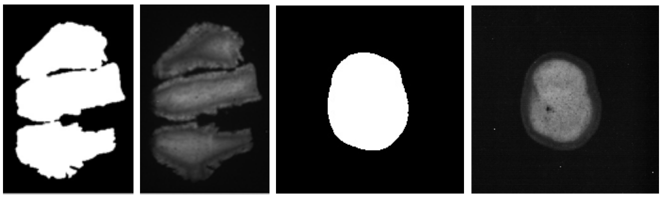

(a) (b) (c) (d)

**Fig. 6** (a) and (b) the ROI and original image of American ginseng, (c) and (d) the ROI and original image of pilose antler.

The whole extracting process of ROI is shown in Figure 7.

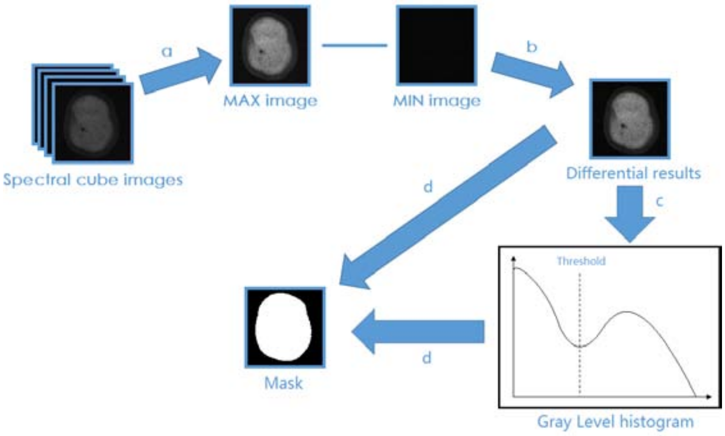


**Fig. 7** Extraction process of ROI

### *3.2 Characteristic Spectral Curve*

The ROI of every image in the spectral cube can be obtained by multiplying the mask. Calculate the average light intensity of the corresponding pixel in ROI and to normalize them according to equation (1), then the characteristic spectral curve and the normalized characteristic spectral curve of the samples can be obtained. Figure 8 shows the characteristic spectral curve of American ginseng and pilose antler.

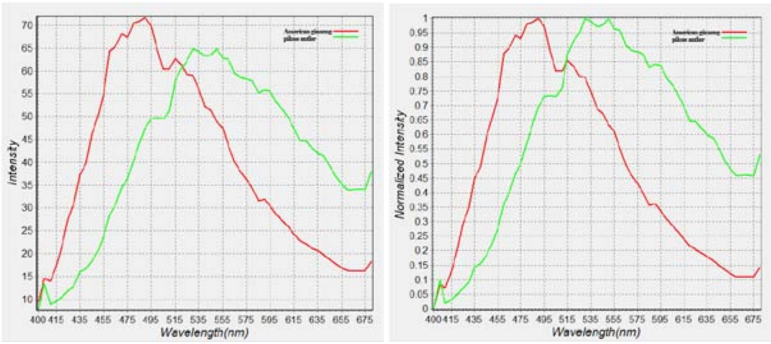


(a) (b)

**Fig. 8** (a) the characteristic spectral curve and (b) the normalized characteristic spectral curve of American ginseng and pilose antler.

## 4 Conclusion

Multispectral imaging is an emerging technology with strong vitality and attractive, and has been used in environment, telemetry, agriculture and other fields. In recent years, this technology is being applied in CMS identification. Extraction of ROI is crux for multispectral imaging to be practically applied in CMS identification. In order to obtain an optimal characteristic spectral curve, different methods for extracting ROI should be employed for different spectral images, but the methods are not fit for real time data analysis. Therefore, a new algorithm for image segmentation is presented. A mask exactly extracting RIO of the multispectral images is generated by the computer automatically by image difference, blurring difference image and threshold determination. The process of the determination of the automatically extracting RIO is described in detail. And multispectral imaging experiments with American ginseng and pilose antler were conducted and more than 95% of the ROI was extracted employing the new algorithm for image segmentation.

This research was supported by Science and Technology Planning Project of Guangdong Province, China, under Grant No. 2012B040302002.

## References

1 Gao JP, Wang YH, Chen DF (2003) Pharmacognostical identification of Chinese crude drug-Fructus Schisandrae Sphenantherae. Chinese Traditional and Herbal Drugs, 34(7):646-649.
2 Xiang ZX, Zeng X, Gao SL (2008) Application and study of HPLC fingerprint of Lonicera japonica for identification of geo-authenticity. China Journal of Chinese Materia Medica, 33(9): 996-998.
3 Kang S, Zhang J, Lin RC (2013) Macroscopic and microscopic characteristics of Chinese Caterpillar Fungus. Acta Pharmaceutica Sinica, 48(3): 428−434.
4 Goetz AFH, Vane G, Solomon TE, et al (1985) Imaging spectrometry for earth remote sensing. Science, 228:.1147-1153.
5 Wu D, Yang H, Chen X (2008) Application of image texture for the sorting of tea categories using multi-spectral imaging technique and support vector machine. Journal of food engineering, .88(3): 474-483.
6 Liang L, Wang L, Pang QC, et al (2012) Study of cortex phellodendri chinensis decoction experiment based on the spectral imaging technology. Spectroscopy and Spectral Analysi, 32(5): 1359-1361.
7 Yang JL, Zhu T, Xu Y (2009) Study on Ultraviolet Fluorescence Spectral of Monomers of Distilled Spirits. Spectroscopy and Spectral Analysi, 29(12): 3339-3343.
8 Zhao J, Ma J, Pang QC, et al (2012) Identification and Analysis of Five Kinds of Chinese Traditional Medicine by Spectral Imaging Technology. Lishizhen Medicine and Material Medica Research, 23(1): 188-190.
9 Meng Q, Pang QC, Ma J, et al (2010) Transmission Spectral Imaging Research on Folium Uncariae from Guangdon. Journal of Chinese Medicinal Material, 33(5): 696~699.
10 Dai C, Pang QC, Ma J, et al (2011). Rapid and Nondestructive Detection of Quality of Panax Quinquefolium Effected by Hunidity. Laser & Optoelectronics Progress, 48(9): 093001-1~093001-7.
11 Wang L, Pang QC, Ma J, et al (2011) A Spectral Image Constructing Method of TCMcs Fluorescent Fingerprints. ACTA PHOTONICA SINICA, Vol.40, No.6, P. 860-864, June 2011.
12 Zhang WX, Pang QC, et al (2010) Self-adaptive region growing algorithm to segment images of spectral imaging for TCM assessment. Journal of Applied Optics, 31(1): 78-82.
13 Zhao J, Pang QC, Ma J, et al (2008) Design of the Continuous Spectrum Imaging Apparatus Based on LCTFs. ,Acta Photonica Sinica, 37(4): 758-762.